eXPRESS Polymer Letters Vol.13, No.3 (2019) 261–275
Available online at www.expresspolymlett.com
https://doi.org/10.3144/expresspolymlett.2019.22

Development of mesoporous polysaccharide/sol-gel composites with two different templating agents: Surfactants and choline chloride-based deep eutectic solvents

V. R. A. Ferreira, M. A. Azenha, A. C. Pinto, P. R. M. Santos, C. M. Pereira, A. F. Silva*

CIQ-UP; Departamento de Química e Bioquímica, Faculdade de Ciências da Universidade do Porto, Rua do Campo Alegre, 4169-007 Porto, Portugal

Received 3 August 2018; accepted in revised form 26 October 2018

Abstract. Mesoporous sorbent composites, evolving from previous work on microporous composites of polyanionic polysaccharides were developed with the purpose of increasing the sorptive features of the materials. Using the widely successful classical surfactant micelle approach, it was observed, in this particular case, that the composites remained essentially microporous. The alternative consisted on the application of deep eutectic solvents (DES). The most common DES (choline chloride + neutral hydrogen bond donor), were tested because of their advantages over other possibilities such as imidazolium-based ionic liquids: lower cost, easy in-house preparation, safe constituents and water stability and solubility. Possible mechanisms underlying the observed mesoporosity were discussed. The surface area ranged between 76 and 267 m^2/g and the average pore size was in the range 3–5 nm. DES had not a negative effect on synthesis yields and, in the case of fucoidan, composites bearing a higher content of the biopolymer were produced. As a consequence and in line with the initial expectations these new composites revealed highly enhanced Pb (II) sorptive features comparatively to their microporous predecessors: chondroitin sulfate composites - up to a 5 fold capacity enhancement; fucoidan composites- up to a 3.5 fold capacity enhancement. The highest capacity was observed for the fucoidan composite prepared with choline chloride-ethyleneglycol DES, 79 mg Pb (II)/g, which is slightly above the highest value (77 mg Pb (II)/g) found in the literature for Pb (II) sorbents based on polysaccharides, sol-gels or their composites.

Keywords: *biocomposites, mesoporosity, chondroitin sulfate, fucoidan, deep eutectic solvent*

1. Introduction

Biodegradable, biocompatible polysaccharides extractable from abundant low-cost raw materials are becoming increasingly appealing for application in different fields of research [1–3]. There is a remarkable diversity of such polysaccharides, many of which are virtually unexplored for their potentialities in the field of metallic cation applications. Namely, the research on negatively-charged sulfated polysaccharides for metal cation-related applications is scarce. The presence of the $–O–SO_3^-$ groups in the structure of these polysaccharides provides them with permanent negatively-charged points even at pH values as low as 2. The eventual cooperativity between sulfate and other nearby functionalities attached to the backbone of the biopolymers foresees strong binding modes towards cationic species with different selectivity from the one associated to the most commonly studied polysaccharides. Probably the major reason for the under-exploitation of sulfated polysaccharides, such as chondroitin sulfate (CS) and fucoidan (Fd), lies in the lack of established procedures of covalent immobilization and reticulation of these water soluble polysaccharides. We tackled the way towards the covalent immobilization of CS and Fd by developing a crosslinking scheme [4] that does not

*Corresponding author, e-mail: mazenha@fc.up.pt

sacrifice the carboxylate/sulfate groups present in the polysaccharide, shown as prevalent in the complexation of metal cations. The process relies on a sol-gel reaction that delivers a rigid microporous biopolymer-silica composite. These composites allowed the exploitation of the negatively-charged CS or Fd for cation recovery from solution, most noticeably Pb (II) [4], an application requiring non-soluble forms of the biopolymer. The composites were also amenable to bioimprinting of Pb (II), a process for the incorporation of a 'memory' effect of the Pb (II) ions, expressed in the observation of stronger (up to 44%) binding as compared to the non-bioimprinted counterparts, and increased selectivity (1.4–2 fold) against Cd (II) [5, 6]. A common feature to all the CS or Fd composites prepared was their microporous structure (N_2 adsorption surface area $\leq$ 17 m^2/g; total pore volume $\leq$ 0.03 ml/g). A network of mesopores would greatly increase the binding surface and therefore render many more binding points accessible to sorbates, even in the inner part of the sorbent particles. This would expectedly increase considerably the capacity of the sorbents and eventually also the binding strength. In addition, mesoporosity is of high importance in other specific areas such as in optics, catalysis, drug delivery systems, coatings, cosmetics, bio-separation, diagnostics, gas-separation and nanotechnology [7]. Initially, we attempted the most common approach of mesoporous templating in sol-gel processes which makes use of surfactants, such as primary amines and quaternary ammonium ions [8–14]. However, as explained later in detail, this approach was hampered by the presence of the biopolymers. We moved then to a more recent approach based on ionic liquids [15]. Imidazolium-based ionic liquids have been widely successfully used for mesoporous templating in sol-gel processes [*e.g.* 16–21]. For example, the preparation and characterization of titania based ionogels synthesized using ionic liquid 1-ethyl-3-methyl imidazolium thiocyanate [20], and the preparation of an ionic liquid-based hydrogel with hyperbranched topology for efficient removal of Cr (VI) [21] have been reported. Nonetheless, we decided to go for an alternative special kind of 'ionic liquids', the deep eutectic solvents (DES) (to be accurate, DES cannot be considered ionic liquids, since not all their constituents are ionic). The most common DES are comprised of choline chloride and a neutral hydrogen bond donor that forms a Lewis adduct with choline and are in use in our labs for some time already [22–25].

The main advantages of DES are the low cost, the easy preparation (without purification, without waste disposal) and the use of safe and common reagents and inert to water (long term stability, easy storage). The application of DES to synthesis has been described mainly for obtaining thermo-resistive materials, carbon materials and porous polymers. These can be used in catalysis, separation and adsorption, for power generation and a multiplicity of other biological applications [26]. The use of DES in polymerization has been considered a greener alternative to conventional syntheses [27–29], very useful for obtaining materials with hierarchical and regular structure. Recently the use of one of these DES to obtain mesoporous sol-gel composites for catalytic purposes [30] has been described.

2. Materials and methods

2.1. Materials

Chondroitin sulfate sodium salt (CS, >90% purity, M_W range 10–100 kDa) was provided by Carbosynth, (Berkshire, UK), extracted from bovine cartilage. Fucoidan (Fd, >90% purity, containing 5% uronic acids, average M_W 73.7 kDa) was provided by Marinova, (Tasmania, Australia), extracted from *Fucus vesiculosus*. Choline chloride (ChCl), Ethylene glycol (EG) and Urea (U) were used for the preparation of DES, which were then used as mesoporosity agents, were obtained from Sigma-Aldrich (Deisenhofen, Germany) with >99% of purity. Hexadecyltrimethylammonium Bromide (CTAB) (Sigma-Aldrich, Deisenhofen, Germany, >99%) and Triton-X 100 (Panreac, Castellar del Vallès, Spain) surfactants were also used as mesoporosous templates. The metal cation salts used in solution for the retention/separation tests, namely $Pb(NO_3)_2$ and $Cd(NO_3)_2 \cdot 6H_2O$, were provided by Merck (Darmstadt, Germany, >99% purity). Glycidyloxypropyl-trimethoxysilane (GPTMS) and tetramethoxysilane (TMOS) were purchased from Sigma-Aldrich (Deisenhofen, Germany) and were used without further purification (> 98%). All other reagents were analytical grade. Water was of Milli-Q (Millipore, Massachusetts, USA) purity.

2.2. Synthesis of composites templated with surfactants

For the CS composites, a CS solution 1.5% *m*/*v* was prepared in deionized water. In a typical synthesis, 20 ml of that solution were mixed with 0.515 ml of pure GPTMS (equivalent to a CS monomer:GPTMS

molar ratio of 1) and the mixture was stirred at room temperature for 17 h. Then, CTAB was added so as to achieve the concentration of 5 mM (above the critical micellar concentration – 1 mM at 25 °C). Immediately upon dissolution of the CTAB, TMOS (CS monomer:TMOS molar ratio 1) was added into the mixture to form a gel after ~2 h. The precipitate was centrifuged at 6000 rpm (PrO-Analitycal, Centurion Scientific Lid CR4000R5 Model, Chichester, UK) for 10 min at 25 °C. The pellet was dried overnight in the oven at 50 °C.

A similar procedure was applied to composites prepared with Triton-X in the place of CTAB. The concentration of surfactant was 50 mM in this case (above the critical micellar concentration – 0.2 mM at 25 °C). The production of Fd composites followed the same procedures.

The surfactants were removed by washing six times with HNO_3 0.01 mol/l. Every washing step was intercalated with centrifugation at 6000 rpm for 10 min. The washings were monitored by analyzing the washed materials by Attenuated Total Reflectance Fourier Transform Infrared (ATR-FTIR) measurements, performed with a Bruker FTIR System Tensor 27 spectrophotometer, with ATR sampling accessory (PIKE MIRacle, Wisconsin, USA) in the range of 600–4000 cm^{-1}.

The acronyms used throughout the remaining text to refer to these composites are composed of the abbreviations of the biopolymer used (CS or Fd) and of the surfactant employed, such as CS_CTAB to indicate the chondroitin sulfate composite prepared in the presence of CTAB.

2.3. Synthesis of composites in DES-containing media

The synthesis was tested with three different choline chloride-based DES:CHCl-Urea (DES-U), CHCl-Ethylene glycol (DES-E) and the mixture of the former two in equal proportion (DES-MIX). DES-U and DES-E were prepared by mixing CHCl with the hydrogen bond donor (urea and ethylene glycol, respectively) in a molar ratio of 1:2 at 60 °C to form a homogeneous liquid. The synthesis involved the preparation of two solutions, one of 1.5% *m*/*v* CS in DES (maximum value of biopolymer solubility) and GPTMS (equivalent to a CS monomer:GPTMS molar ratio of 1), and another of 2% (*v*/*v*) TMOS in 0.01 M HNO_3. After 17 h of stirring the CS/GPTMS solution, the two solutions were mixed in equal proportion in volume (typically a final volume of 30 ml) forming a gel after ~4 h. The precipitate was centrifuged at 6000 rpm for 10 min at 25 °C. The pellet was dried overnight in the oven at 50 °C. The same procedure was followed for the production of Fd composites.

DES were removed by washing with deionized water with stirring for 5 plus 10 minutes of ultrasound. Every washing step was intercalated with centrifugation at 6000 rpm for 10 min. The washings were monitored by ATR-FTIR in the range of 600–4000 cm^{-1}.

The acronyms used throughout the remaining text to refer to these composites are composed of the abbreviations of the biopolymer used (CS or Fd) and of the DES employed, such as CS_DES-U to indicate the chondroitin sulfate composite prepared in a medium containing choline chloride-urea.

2.4. Characterization of the composites

The degree of swelling (S_w) of composites were determined by a method already described in the literature [4] taking into account the differences in dry mass (30 mg) and wet mass after 24 h contact with 1 ml of deionized water (pH 7).

The surface area and pore parameters were determined by a nitrogen adsorption analyzer (TriStar Plus, Micromeritics, Norcross, USA). All samples were pre-treated and analyzed following conditions previously described in the literature [4]. To obtain the specific surface area (S) data was adjusted to the BET model, the specific pore volume (V_p) was obtained by the Gurvitch method and the average pore diameter (D_p) through the BJH theory applied to the desorption branch of the isotherm.

The amount of CS/Fd present in the all composites was determined indirectly using a turbimetric method described in the literature [31]. This method is based on the precipitation reaction between the sulfate groups of CS and Fd with Ba^{2+}, followed by turbidimetric analysis (Portable Turbidimeter 2100Qis, HACH). In this way, it was possible to quantify the remaining biopolymers in the supernatant of the reaction mixture. Thermal gravimetric analysis (TGA), conducted on a Hitachi, Model STA 7200 RV Analyzer (Tokyo, Japan) from room temperature to 800 °C with a heating rate of 10 °C·min^{-1} under a nitrogen flow, was also used for the determination of biopolymer fraction in the composites synthetized in DES-containing media. The quantification was based on the analysis of the individual biopolymers, the sol-gel

control, and the respective biocomposites. Assuming that the thermal behavior of the components present in the composite is similar to their behavior in the individual state, the following system of Equations (1) was used to determine the biopolymer quantity in the composites obtained:

$$\begin{cases} \text{lost mass}_{\text{biocomposite}} = x \cdot m_{\text{biopolymer}} + y \cdot m_{\text{sol-gel}} \\ \text{total mass}_{\text{biocomposite}} = m_{\text{biopolymer}} + m_{\text{sol-gel}} \end{cases} \quad (1)$$

where x corresponds to the mass fraction lost at 800 °C at individual biopolymer analysis; y corresponds to the mass fraction lost at 800 °C at sol-gel control analysis; *lost mass*$_{\text{biocomposite}}$ [mg] corresponds to the mass of the biocomposite lost at 800 °C and *total mass*$_{\text{biocomposite}}$ [mg] to the initial mass of biocomposite; all these masses were corrected by subtracting the amounts of the solvent, estimated from the first mass loss event of every TGA curve.

A Thermo Fisher Scientific Quanta 400FEG ESEM/EDAX Genesis X4M (Hilsboro, OR, USA) scanning electron microscope (SEM), was used to visualize the surface morphology of the biocomposites, at CEMUP, University of Porto. The samples were coated with a Au-Pd film prior to analysis.

2.5. Batch sorption studies: Isotherms and kinetics

The sorption assays performed, followed the conditions described in the literature for batch sorption experiments [4]. The biocomposite (10 mg) was exposed to 5 ml of acetate buffer supplemented with different concentrations of each metal cation, in a range of 4 to 100 mg/l (individual cation solutions were used in these studies). Sorption kinetics were determined by aliquots collected at regular intervals up to 6 h. Once the equilibration time was established (6 h), the isotherms of all samples were determined. All experiments were conducted under stirring (120 rpm) and at constant temperature (25 °C). Finally, all samples were centrifuged at 6000 rpm for 10 min at 25 °C. The supernatant was acidified to pH 4 with concentrated nitric acid and stored protected from light, until Atomic Absorption analysis (Perkin Elmer, AAnalyst 200 model, Waltham, USA, operated at the instrumental parameters recommended by the manufacturer for every element analyzed).

Non-linear fitting of theoretical isotherms to experimental data was performed using IGOR PRO software Package. In this study, three models, Langmuir (Equation (2)), Freundlich (Equation (3)) and Langmuir-Freundlich isotherms (L–F) (Equation (4)), were tested to describe the sorption of the metallic cations:

$$q_e = \frac{q_{\max} KC}{1 + KC} \quad (2)$$

$$q_e = \alpha C^m \quad (3)$$

$$q_e = \frac{q_{\max} (KC)^m}{1 + (KC)^m} \quad (4)$$

where q_e corresponds to the sorbed concentration in equilibrium [mg/g]; C is the equilibrium concentration in solution [mg/l] and α and m are fitting constants. The constant α is related with the binding affinity and the parameter m refers to the heterogeneity index and its value ranges from 0 to 1, increasing as heterogeneity decreases.

Sorption kinetics fitting was tested by linear regression using pseudo-first order (Equation (5)) and pseudo-second order (Equation (6)) models:

$$q_t = q_e (1 - e^{kt}) \quad (5)$$

$$q_t = \frac{q_e^2 kt}{1 + q_e kt} \quad (6)$$

where q_t is the amount of each compound biosorbed at time t [mg/g], and k is the rate constant of each model.

3. Results and discussion

3.1. Mesoporous templating schemes

The theoretical principle underlying the use of surfactants in mesoporous templating is that the formation of micelles during the networking process will leave mesopores after their removal (Figure 1). In the present work two surfactants, one cationic (CTAB) and one neutral (Triton-X) were tested as mesoporous templating agents for Fd and CS composites. In the case of Fd composites, only with the neutral surfactant was possible to observe the formation of a brownish composite gel after 2 days of reaction. With CTAB there was no gelation, not even after a week of reaction, indicating the non-effectiveness of the formation of bridges between polymeric chains, though they are known to be effective in the absence of CTAB [4]. Since Fd contains 3 –SO_3^- groups per structural unit, it is highly charged (negatively) and is expected

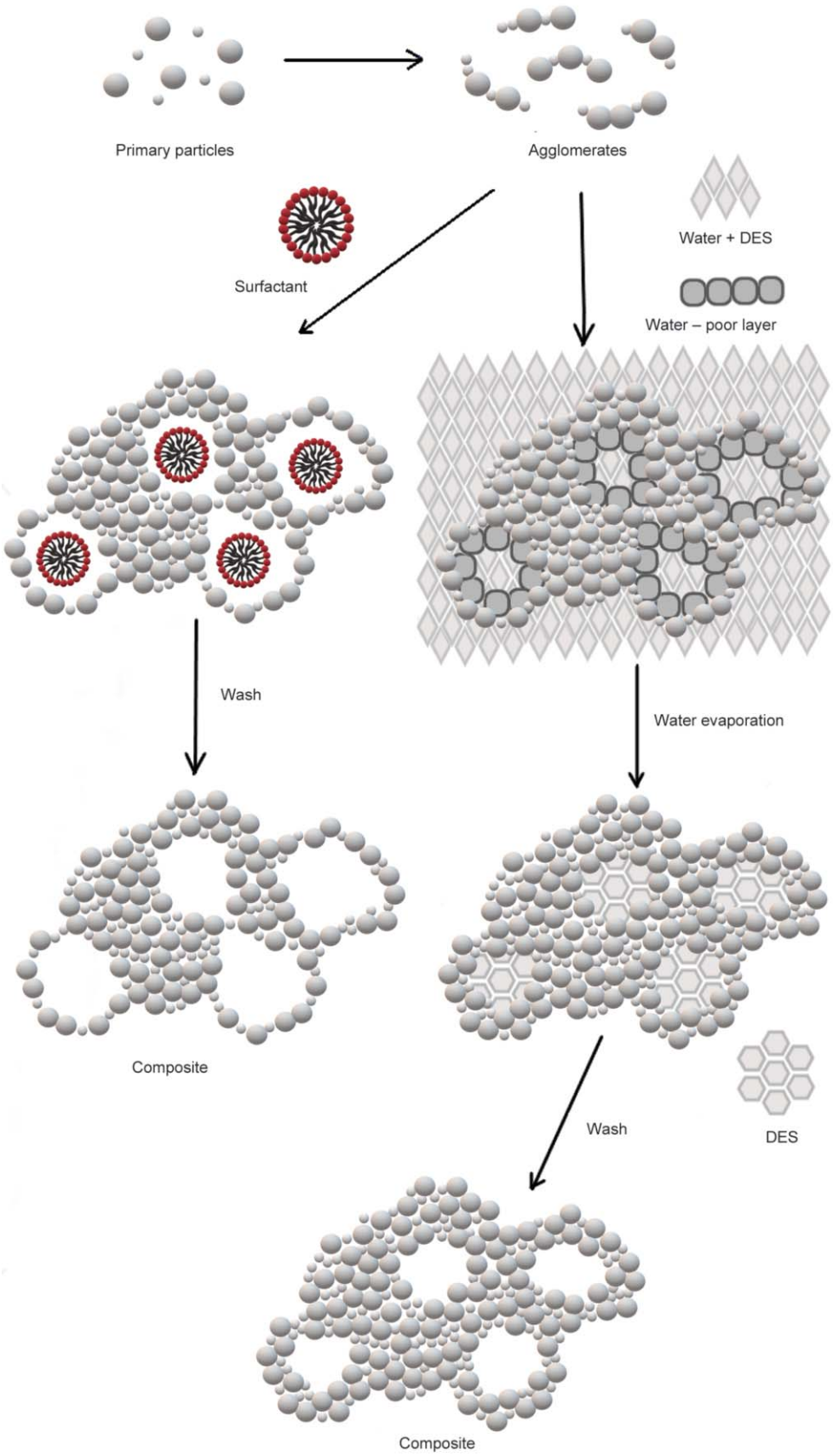

Figure 1. Synthesis routes of mesoporous materials using DES and surfactant (as template). In the case of DES route, two hypothesized mechanisms are shown in sequence, although in reality they may occur independently from each other or in a sinergistic way (cf. text for the detailed discussion).

to display strong attractive interactions with the cationic surfactant. These interactions probably led to Fd_CTAB entangled structures which prevented the crosslinking reactions from taking place. In contrast, with CS (containing only one sulfate group per CS unit, in average) the use of CTAB and Triton-X resulted, after two days of reaction, in composites in the final form of a white powder. However, the use of Triton-X was abandoned due to the low synthesis yields (<30%). Therefore, only Fd/Triton-X- and CS/CTAB-based composites were considered for the subsequent experiments.

Concerning the ionic liquids (IL), some proposed mechanisms for mesoporosity relied on σ-bonding involving the IL ions and the sol initial aggregates, leaving the preferential π orientation for the stacking of IL [32]. However, the choline chloride DES used here present no appreciable π stacking capability. Moreover, due to a question of solubilisation of all the components and because it is one of the sol-gel reagents, a volume of water was required in the final mixture (50% in volume in this case). The presence of water brings the question of whether the molecular structure of the DES, based on hydrogen bonding, is disrupted up to an extent that the DES components are mostly solvated by water, and thus the DES is not present in the mixture as such. This is an open research issue, but considering the available information on DES/water mixtures found in the literature [33, 34], it appears likely that disruption of the DES is what happens here. Nevertheless, based on other mechanisms already proposed in the literature, we had expectations that the DES properties could be effective for the development of mesoporosity in our aqueous/DES mixtures. These rested on two possibilities. The first of them consists of the capping effect of DES components around the sol/biopolymer particles, forming a water poor layer, as proposed in [35]. The effect of such layer would be the retardation of ageing and complete condensation before water evaporation, allowing the formation of a stable gel-DES network, enabling the ulterior DES extraction without gel shrinkage (Figure 1). The second one, proposed for the preparation of mesoporous silica in a choline chloride/urea DES medium also containing water [30], and perhaps the one most likely applicable here, considers that the ageing of the gels at a temperature below that of the degradation of the DES components will remove water and leave the time for the formation of a robust structure due to the condensation of silanols around the DES filler (Figure 1). This possibility is compatible with our process of synthesis, comprising an ageing period at 50 °C before extracting out the remaining DES filler. The concomitance of the two mechanisms is seemingly possible and would also result in the formation of a mesoporous network. Regardless of the actual mechanisms underlying the process, using any of the three different choline chlorides, it was indeed possible to obtain both CS and Fd composites, as described next.

3.2. Structural and chemical characterization of CS and Fd composites.

The composition of the produced materials was evaluated by the identification of ATR-FTIR spectral bands assigned to the characteristic functional groups (Figure 2).

Foot and Mulholland [36] refer to absorption bands 1671 cm^{-1} (C=O of CS amide), 1584 cm^{-1} (C-N of CS amide), as the main recognition bands of CS, while Choi *et al*. [37] characterize the Fd with the absorption bands at 1423 and 1399 cm^{-1} (COO carboxyl groups), indicating the possibility of the band at

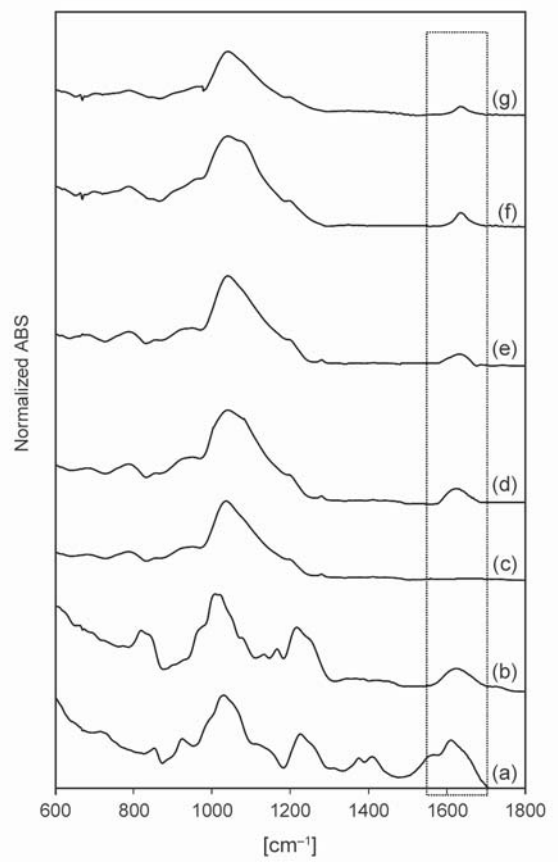

Figure 2. Normalized ATR-FTIR spectra of: a) CS; b) Fd; c) pure sol-gel material; d) CS_DES-E; e) CS_CTAB; f) Fd_Triton-X and g) Fd_DES-E.

1687 cm^{-1} (C=O carbonyl groups of Fd; corresponding to possible impurities of alginic acid or uronic acids bound to the structure of Fd). These bands were identified in spectra of pure CS (Figure 2 curve a) and pure Fd (Figure 2 curve b). In addition, there is the absorption band at 1258 cm^{-1} (S=O of CS and Fd sulfate groups). Comparing with pure sol-gel reference spectrum (Figure 2 curve c), none of these bands has been identified. Therefore, by comparing the spectra of CS-containing gels (Figure 2 curves d and e) and those containing Fd (Figure 2 curves f and g) with the spectrum in Figure 2 curve c (control), it was possible to confirm the presence of polymer and sol-gel components of the materials produced both with surfactants and DES. Specifically, these spectra exhibited the peak at ~1680 cm^{-1}, distinctive of CS and Fd, and the more intense peak of silica at ~1170 cm^{-1}.

Once detected, the contents of CS/Fd present in the composites were determined indirectly by quantifying the amount of biopolymer remaining in the supernatant after the synthesis, applying the turbidimetric method described in the section 2.4. In the case of the composites prepared with DES, the quantification of biopolymer fraction was also performed by thermogravimetric analysis (TGA), which constitutes a direct, more reliable method. The relative proportion of biopolymer in the CS composite gels was estimated in the ranges 40–44% (turbidimetry, indirect method) and 44–49% (TGA, direct method), and for the Fd composites in the ranges 42–52% (turbidimetry) and 53–60% (TGA) (Table 1). The agreement between the two methods was reasonable, especially for the CS composites, implicating that the turbidimetric approach may be used as a faster and cheaper alternative to TGA, as a rough estimate on a routine basis. Anyway, these composites contained similar or higher biopolymer contents as compared to their previous microporous counterparts [4]. These are significant levels of biopolymer (CS/Fd) in the final composites, providing the desirable abundance of anionic interaction points. For the CS_CTAB, the biopolymer content was much lower (23%, turbidimetric method), possibly due to the difficulty in establishing bridges between polymeric chains, derived from the presence of the positively charged surfactant. In the case of the Fd composite prepared with Triton-X it was not possible to quantify the biopolymer content by turbidimetry, since the surfactant interferes severely with the quantification procedure.

The BET specific surface area (S) and the specific pore volume (V_p) were calculated from the nitrogen adsorption isotherms and were also summarized in Table 1. The texture results, characterized by low surface area (1–34 m^2/g) and low pore volume (0.004–0.08 ml/g) for the CS_CTAB and Fd_Triton-X composites, indicate an essentially microporous compacted structure (Figure 3). However, for the CS_Triton-X composite it was possible to obtain a significant volume of mesopores (0.08 ml/g) with average size of 3.6 nm in diameter. In this case it appears that micelles were indeed formed and incorporated into the composite network, providing the desired mesoporous templating effect, although not in the extensive fashion usually reported for simpler sol-gel synthesis [12, 38]. In fact, the majority of the studies present the formation of micelles in aqueous matrices with silicates and other basic components, not with biopolymers, as is the case. The difficulty/impossibility of obtaining mesopores was possibly a consequence of the inability of these surfactants to form micelles in such a complex matrix, as has been reported in the literature for similar mixtures [39]. Furthermore, in the particular case of CTAB (cationic

Table 1. Microstructural properties and biopolymer contents of the composites.

Composites	BET						Mass fraction of CS or Fd in composites				Swelling [%]	
	Surface area [m^2/g]		Pore volume [ml/g]		Pore size [nm]		Indirect analysis – Turbidimetry		Direct analysis – TGA			
	CS	Fd	CS	Fd	CS	Fd	CS	Fd	Cs	Fd	CS	Fd
DES-U	267	78	0.23	0.06	3.4	3.6	0.42	0.42	0.44	0.57	72	54
DES-E	178	76	0.23	0.09	4.4	4	0.40	0.52	0.45	0.53	59	77
DES-MIX	208	266	0.25	0.33	3.9	4.6	0.44	0.42	0.49	0.60	48	81
CTAB	14	–	0.03	–	<2	–	0.23	–	–		86	–
Triton-X	34	1	0.08	0.004	3.6	<2	–		–		156	163
Without surfactant or DES*	9	6	0.03		<2		0.45	0.34			3	2

*Data taken from [4].

surfactant), strong electrostatic interactions with the biopolymer (anionic) may occur, making it impossible to form micelles, hence the low number (even nonexistence) of mesopores [40]. On the other hand, the composites synthesized in DES-containing media, in general, presented much higher surface area (76–267 m^2/g) and pore volume (0.06–0.25 ml/g), as was aimed at (representative adsorption isotherms and pore distribution profiles are presented in Figure 3). It appears then that the choline chloride-based DES were effective in the development of mesoporosity within the sol-gel/biopolymer composites. Observing the biocomposite particles at the scanning electron microscope (SEM), mesopores could be perceived

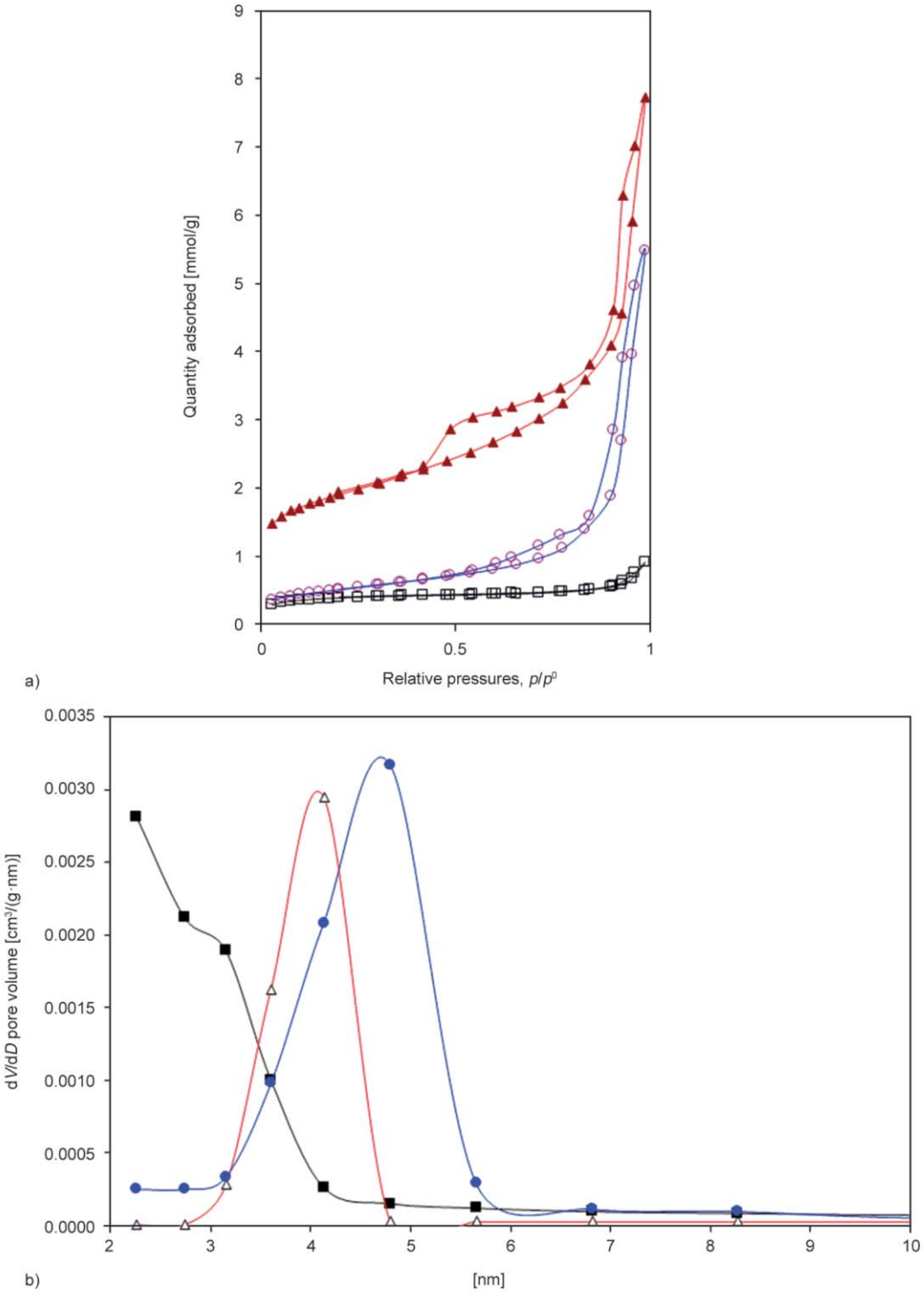

Figure 3. Surface characterization: a) N_2 adsorption isotherms and b) pore size distribution typically obtained ((▲) CS_DES-MIX, (●) Fd_DES-MIX and (■) Fd_Triton-X).

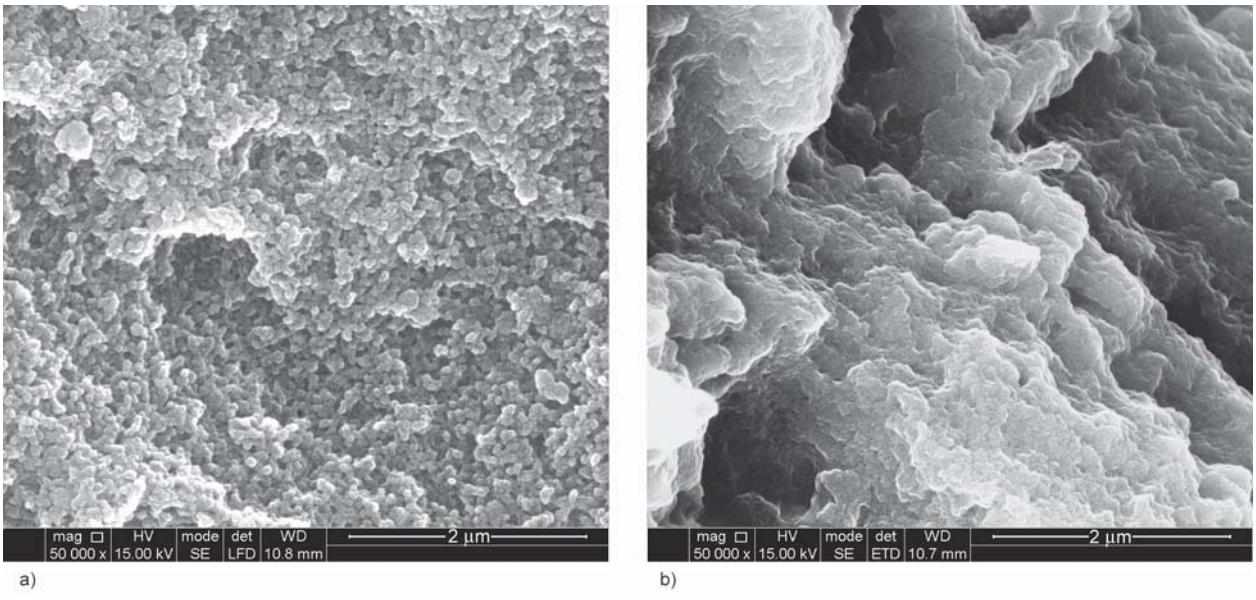

Figure 4. Representative SEM micrographs of a) CS_DES-MIX and b) Fd_DES-MIX composites.

(Figure 4), especially for the CS composites, but only those much larger (>10 nm) than the predominant sizes given by the N_2 adsorption measurements (3–5 nm), which are beyond the resolution of SEM. The micrographs revealed, as a general rule, different textures for the CS and Fd composites. While the CS composites appeared to form essentially by aggregation of sub-microparticles, the Fd composites, at the same scale, appeared as a continuous, layered body. Anyhow, in both cases, the mesoporous network is expected to translate into improved sorptive properties, as addressed in the next section.

The degree of swelling (S_w) in water was determined in order to complement information regarding the physical structure of the composite network and the mechanical stability. The degree of swelling depends on the sample-solvent interaction, degree of crosslinking of the sample itself, the pore volume and the biopolymer content. Analyzing the results in Table 1 it is possible to verify that most of the swelling values were within the range 48–86%, compatible with stable and strongly crosslinked gels. The composites prepared in the presence of Triton-X presented much higher swelling (>150%), most likely due to a lower crosslinking degree or weaker (non-covalent) crosslinking connections, as deduced from the observed loss of composite mass during the tests in aqueous media.

Overall, considering the clear superiority of the DES-templated synthesis in terms of mesoporosity and also due to higher yields and biopolymer contents, it was decided at this point to discard completely the surfactant templated approach from the present study.

3.3. Sorption isotherms and kinetics

For an insight into the sorption properties of mesoporous materials, such as kinetics, capacity, affinity constant, and heterogeneity index, kinetics and isotherms models were applied to the data obtained experimentally from the batch studies described in 2.5. The tested sorbates were Pb (II) and Cd (II) (isotherms only), in line with our previous studies [4–6].

The kinetic profiles obtained for the sorption of Pb (II) on the mesoporous materials are shown in Figure 5. In general, smooth profiles were obtained showing a continuous decrease of the incremental sorption over time to a maximum equilibrium amount. The equilibrium, in the CS materials was obtained after 4 h or less, whereas a faster sorption was observed for the Fd materials (equilibrium hit two hours earlier). To ensure equilibrium, 6 h was the mixing time fixed for the following studies of equilibrium isotherms. Concerning the fitting of the kinetics data to the pseudo-first order (Equation (5)) and pseudo-second order (Equation (6)) models, the selection of the most adequate one was made according to the higher correlation coefficient values obtained. The pseudo-second order model fitted globally better to the sorption of all mesoporous materials ($r^2 > 0.98$). As demonstrated by Azizian [41] the pseudo-second order sorption kinetics is applicable when the initial concentration of the sorbate is not too high against

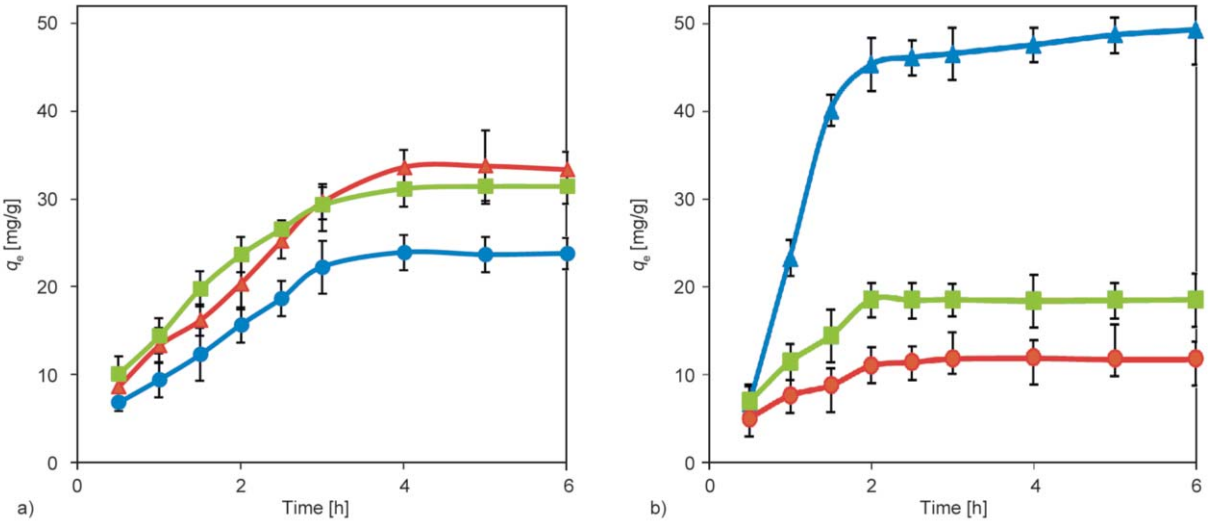

Figure 5. Kinetic profiles of Pb (II) sorption (C_i = 60 mg/l) by a) CS_DES composites and b) Fd_DES composites: (■) DES-MIX, (▲) DES-E and (●) DES-U. Error bars represent the standard deviation of the mean result (n = 3).

another rate-law parameter dependent on the sorbent capacity. The fitting parameters are presented in Table 2. It may be perceived from both Figure 5 and Table 2 that the sorption of Pb (II) with CS composite (*k:* 0.9–1.3 g/(mg·min^{-1}) occurred significantly slower than with Fd composite (*k:* 1.9–2.7 g/(mg·min^{-1})) independently of the DES used. Comparing with the corresponding microporous materials (*k* approx. 1 g/(mg·min^{-1})) [4] there is a 2–3 fold increase in the sorption rate of the Pb (II) in Fd composites, remaining similar in the CS composites. Regarding the sorption isotherms, the data points (q_e, C) obtained (Figure 6) were fitted to the different isotherm models, such as Langmuir (Equation (2)), Freundlich (Equation (3)) and hybrid L–F (Equation (4)) by non-linear regression analysis. The

Table 2. Isotherms and sorption kinetics models fitting parameters.

DES	Biopolymer	Sorbate	Langmuir-Freundlich isotherm model*			Sorption kinetics (C_i = 60 mg/l) Model pseudo second order**	
			K [l/mg]	q_{max} [mg/g]	m	k [g/mg·min^{-1}]	q_e [mg/g]
DES-E	CS	Pb (II)	328±24	55±2	0.96±0.05	0.9±0.1	32±2
		Cd (II)	311±44	51±3	0.91±0.04	–	–
	Fd	Pb (II)	347±24	79±2	0.94±0.05	2.7±0.1	49±2
		Cd (II)	105±44	40±3	0.88±0.04	–	–
DES-U	CS	Pb (II)	375±28	54±3	0.95±0.07	1.3±0.1	33±3
		Cd (II)	347±21	50±1	0.91±0.03	–	–
	Fd	Pb (II)	27±24	14±2	0.71±0.05	2.2±0.1	12±2
		Cd (II)	32±44	14±3	0.63±0.04	–	–
DES-MIX	CS	Pb (II)	439±46	61±5	0.97±0.04	1.2±0.6	24±3
		Cd (II)	378±41	60±3	0.95±0.05	–	–
	Fd	Pb (II)	201±24	59±2	0.84±0.05	1.9±0.1	19±2
		Cd (II)	142±44	32±3	0.81±0.04	–	–
Without DES***	CS	Pb (II)	230±37	12±2	0.97±0.04	1.1±0.6	5±1
		Cd (II)	105±18	11±2	0.95±0.04	3.5±0.8	4±1
	Fd	Pb (II)	370±33	24±3	0.98±0.01	1.0±0.5	10±3
		Cd (II)	140±21	21±2	0.95±0.04	2.1±0.6	10±2

*Non-linear fitting exhibiting $\chi^2 < 10^{-7}$

**Model fitting by linear regression exhibiting $r^2 \geq 0.998$ in every instance.

***Data taken from [4]

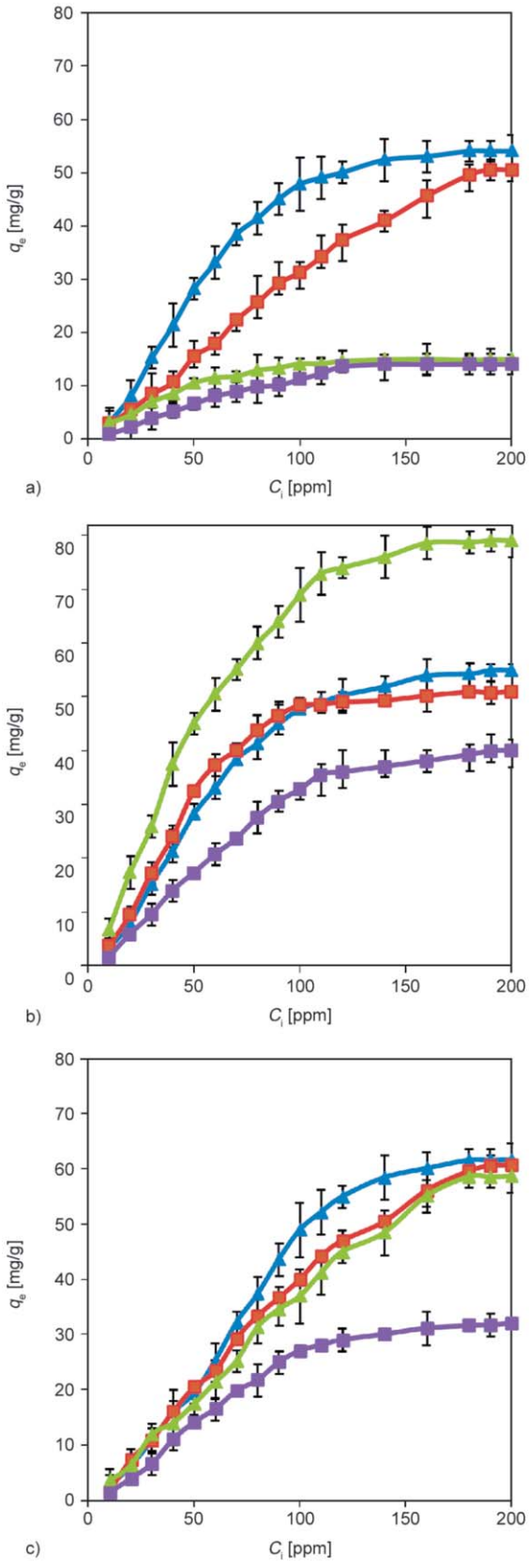

Figure 6. Equilibrium binding isotherms for the sorption Pb (II) (▲) and Cd (II) (■) by CS and Pb (II) (▲) and Cd (II) (■) by Fd composites: a) DES-U, b) DES-E, c) DES-MIX. Error bars represent the standard deviation of the mean result (n = 3).

best fitting was selected according to the lowest χ^2 (chi-squared) values obtained and q_e proximity between the calculated values and the experimental values. In all cases the L–F model provided the best fit. The corresponding isotherm parameters were condensed in Table 2. The L-F model assumes that the sorption behavior varies with the initial concentration of the sorbate. At lower sorbate concentrations this model approaches the Langmuir isotherm while at higher concentrations it approaches the Freundlich model. The L-F model has the advantage of allowing the determination of the saturation capacity (q_{max}), the affinity constant and the degree of heterogeneity (m). The capacities of CS and Fd composites, expressed in terms of mass, were higher for Pb (II) (54–61 mg/g of CS composites, 59–79 mg/g of Fd composites) than for Cd (II) (50–60 mg/g of CS composites, 32 and 40 mg/g of Fd composites), reflecting the known natural selectivity of the different materials for the cation Pb (II) [4]. The retention capacities of Pb (II) reported for other mesoporous sorbents based on polysaccharides and silicates [42], cover a wide range from 18 to 77 mg/g as is it possible to verify in Table 3. The capacities found for our composites CS/Fd fall near the upper end or above that capacity range, indicating the sorption effectiveness of the new materials. It may be stated that the dramatic increase of sorption capacity, in comparison with the microporous counterparts (11–12 mg/g of CS composites, 21–24 mg/g of Fd composites), was due mainly to the development of the mesoporous network, although in the case of Fd composites the higher fraction of biopolymer in the composite must have had a contribution too. An exception to all this was found for the Fd_DES-U composite, which presented capacity values and affinity constants for Pb (II) and Cd (II) much lower than the other materials. These surprising results were confirmed to be reproducible and will require further research in order to reach a sound elucidation. In general, the composites exhibiting higher capacities for Pb (II) also expressed the highest affinity constants (328–439 and 201–347 l/mg for CS and Fd composites, respectively). In the case of CS composites, the affinity constants for Cd (II) (311–378 l/mg) were slightly lower than those for Pb (II). For the Fd composites the Cd (II) affinity constants (105–142 l/mg) were considerably lower (1.5–2.5 fold) than those for Pb (II). It appears that the DES-templated CS composites may have acquired a different selectivity profile for heavy metal

Table 3. Sorption capacity of Pb (II) and textural features presented by mesoporous materials based in silica and biopolymers, described in the literature.

Sorbents	q_{max} [mg/g]	Surface area [m^2/g]	Pore volume [cm^3/g]	Pore size [nm]	Ref.
Chitosan beads	26.1	501.6	–	12.9	[43]
Chitosan-GLA beads	14.2	617.2		12.7	[43]
Chitosan-alginate beads	24.3	447.5		16.3	[43]
Thiol-functionalized magnetic mesoporous silica material	22.3	321.1	0.29	2.5	[44]
Magnetic chitosan/graphene oxide	76.9	382.5	0.40	2.8	[45]
Mesoporous silica	57.7	–			[46]
Mesoporous silica SBA-15	38.1	546.3	0.82	6.6	[47]
Pb (II)-IIP unleached	22.7	100.8	0.12	2.6	[47]
Pb (II)-IIP ion-imprinted polymer	18.4	113.8	0.27	3.9	[47]

cations (in binding strength), as judging by the Pb (II)/Cd (II) pair only and the results of our previous research [5, 6]. This may be related to different conformational arrangements acquired by the CS chains during the DES-templated synthesis. All the composites (except Fd_DES-U) presented a homogeneous distribution of the sorption sites ($m \approx 1$), indicating that the mesoporous network growth process was able to homogeneously distribute the constituents of the synthesis in order to create a set of sorption points with equal affinity for the different metals, suggesting that the metals were able to interact with well-defined sorption sites.

The possibility of regeneration of the composites, upon the sorption of the cations, is also an important feature of the sorbents [48]. It was observed that the quantitative recovery of the metals was achieved with acidic washes (0.01 mol/l HNO_3). However, the maximum number of possible sorption-wash cycles was not ascertained.

4. Conclusions

The application of surfactant micelles as mesoporous templates was unsuccessful in the conditions of synthesis of chondroitin sulfate or fucoidan sol-gel composites. The strong interactions between the surfactants and the polyanionic biopolymers appear to have impeded both the formation of micelle and the biopolymer-sol-gel precursor connectivity. Conversely, the incorporation of deep eutectic solvents into the reacting mixture resulted in the production of composites exhibiting mesoporous features: surface area ranging 76 to 267 m^2/g, pore size in the range 3.4–4.6 nm. The mesoporosity probably originated at the ageing stage (evaporation of water – formation of DES filler), which may also have had the contribution from a capping effect around the sol/biopolymer particles and inside the pores, which, overall, prevented gel shrinkage. Due to their lower cost and easier preparation relatively to the ionic liquids already being employed for mesoporous templating, the deep eutectic solvents may thus become an advantageous alternative. In fact, the mesoporous composites developed in our study generally revealed sorptive features clearly above the average features found for other Pb (II) sorbents based on polysaccharides, sol-gels or their composites. Additionally, these composites exhibited highly enhanced sorptive features comparatively to their microporous predecessors: CS composites – up to a 5 fold capacity enhancement, Fd composites – up to a 3.5 fold capacity enhancement. Furthermore we intend to find even greater Pb (II) sorption abilities in future composites prepared in the presence of deep eutectic solvents, subjected to a bioimprinting process.

Acknowledgements

This work was financed by the European project NANOCOATIL – High performance nanostructured coatings using ionic liquids based on choline chloride (M-ERA-NET/009/2012). VF is grateful to the Portuguese Foundation for Science and Technology (FCT) for the scholarship SFRH/BD/126642/2016.

References

[1] Reddy H. K., Lee S. M.: Application of magnetic chitosan composites for the removal of toxic metal and dyes from aqueous solutions. Advances in Colloid and Interface Science, **201–202**, 68–93 (2013). https://doi.org/10.1016/j.cis.2013.10.002

[2] Bailey S. E., Olin T. J., Bricka R. M., Adrian D. D.: A review of potentially low-cost sorbents for heavy metals. Water Research, **33**, 2469–2479 (1999). https://doi.org/10.1016/S0043-1354(98)00475-8

[3] Yu B., Yang B., Li G., Cong H.: Preparation of monodisperse cross-linked poly(glycidyl methacrylate)@Fe_3O_4@diazoresin magnetic microspheres with dye removal property. Journal of Materials Science, **53**, 6471–6481 (2018). https://doi.org/10.1007/s10853-018-2018-9

[4] Ferreira V. R. A., Azenha M. A., Bustamante A. G., Mêna M. T., Moura C., Pereira C. M., Silva A. F.: Metal cation sorption ability of immobilized and reticulated chondroitin sulfate or fucoidan through a sol-gel cross-linking scheme. Materials Today Communications, **8**, 172–182 (2016). https://doi.org/10.1016/j.mtcomm.2016.08.003

[5] Ferreira V. R. A., Azenha M. A., Pereira C. M., Silva A. F.: Preparation and evaluation of Pb(II)-imprinted fucoidan-based sorbents. Reactive and Functional Polymers, **115**, 53–62 (2017). https://doi.org/10.1016/j.reactfunctpolym.2017.04.001

[6] Ferreira V. R. A., Azenha M. A., Mêna M. T., Moura C., Pereira C. M., Pérez-Martín R. I., Vázquez J. A., Silva A. F.: Cationic imprinting of Pb(II) within composite networks based on bovine or fish chondroitin sulfate. Journal of Molecular Recognition, **31**, 2614–2623 (2018). https://doi.org/10.1002/jmr.2614

[7] Tripathi A. K., Singh R. K.: Immobilization induced molecular compression of ionic liquid in ordered mesoporous matrix. Journal of Physics D: Applied Physics, **51**, 075301/1–075301/12 (2018). https://doi.org/10.1088/1361-6463/aaa56c

[8] Nemanashi M., Noh J. H., Meijboom R.: Dendrimers as alternative templates and pore-directing agents for the synthesis of micro- and mesoporous materials. Journal of Materials Science, **53**, 12663–12678 (2018). https://doi.org/10.1007/s10853-018-2527-6

[9] Peshoria S., Narula A. K.: Structural, morphological and electrochemical properties of a polypyrrole nanohybrid produced by template-assisted fabrication. Journal of Materials Science, **53**, 3876–3888 (2018). https://doi.org/10.1007/s10853-017-1769-z

[10] Pal N., Bhaumik A.: Soft templating strategies for the synthesis of mesoporous materials: Inorganic, organic–inorganic hybrid and purely organic solids. Advances in Colloid Interface Science, **189–190**, 21–41 (2013). https://doi.org/10.1016/j.cis.2012.12.002

[11] Mehmood A., Ghafar H., Yaqoob S., Gohar U. F., Ahmad B. J.: Mesoporous silica nanoparticles: A review. Journal of Developing Drugs, **6**, 174–184 (2017). https://doi.org/10.4172/2329-6631.1000174

[12] Yang H., Xu R., Xue X., Li F., Li G.: Hybrid surfactant-templated mesoporous silica formed in ethanol and its application for heavy metal removal. Journal of Hazardous Materials, **152**, 690–698 (2008). https://doi.org/10.1016/j.jhazmat.2007.07.060

[13] Lu Q., Chen D., Jiao X.: Fabrication of mesoporous silica microtubules through the self-assembly behavior of β-cyclodextrin and Triton-X-100 in aqueous solution. Chemistry of Materials, **17**, 4168–4173 (2005). https://doi.org/10.1021/cm0501564

[14] Cao L., Xu L., Zhang D., Zhou Y., Zheng Y., Fu Q., Jiang X. F., Lu F.: D-A dyad and D-A-D triad incorporating triphenylamine, benzanthrone and perylene diimide: Synthesis, electrochemical, linear and nonlinear optical properties. Chemical Physics Letters, **682**, 133–137 (2017). https://doi.org/10.1016/j.cplett.2017.06.015

[15] Sachse A., Wuttke C., Díaz U., de Souza M. O.: Mesoporous Y zeolite through ionic liquid based surfactant templating. Microporous and Mesoporous Materials, **217**, 81–86 (2015). https://doi.org/10.1016/j.micromeso.2015.05.049

[16] Sanaeishoar H., Sabbaghan M., Mohave F.: Synthesis and characterization of micro-mesoporous MCM-41 using various ionic liquids as co-templates. Microporous and Mesoporous Materials, **217**, 219–224 (2015). https://doi.org/10.1016/j.micromeso.2015.06.027

[17] Hu J., Gao F., Shang Y., Peng C., Liu H., Hu Y.: One-step synthesis of micro/mesoporous material templated by CTAB and imidazole ionic liquid in aqueous solution. Microporous and Mesoporous Materials, **142**, 268–275 (2011). https://doi.org/10.1016/j.micromeso.2010.12.011

[18] Bhadani A., Misono T., Singh S., Sakai K., Sakai H., Abe M.: Structural diversity, physicochemical properties and application of imidazolium surfactants: Recent advances. Advances in Colloid and Interface Science, **231**, 36–58 (2016). https://doi.org/10.1016/j.cis.2016.03.005

[19] Fu J., Lu Q., Shang D., Chen L., Jiang Y., Xu Y., Yin J., Dong X., Deng W., Yuan S.: A novel room temperature POSS ionic liquid-based solid polymer electrolyte. Journal of Materials Science, **53**, 8420–8435 (2018). https://doi.org/10.1007/s10853-018-2135-5

[20] Verma Y. L., Tripathi A. K., Shalu, Singh V. K., Balo L., Gupta H., Singh S. K., Singh R. K.: Preparation and properties of titania based ionogels synthesized using ionic liquid 1-ethyl-3-methyl imidazolium thiocyanate. Materials Science and Engineering B, **220**, 37–43 (2017). https://doi.org/10.1016/j.mseb.2017.03.010

[21] Li K., Qian L., Song W., Zhu M., Zhao Y., Miao Z.: Preparation of an ionic liquid-based hydrogel with hyperbranched topology for efficient removal of Cr(VI). Journal of Materials Science, **53**, 14821–14833 (2018). https://doi.org/10.1007/s10853-018-2609-5

[22] Pereira N. M., Pereira C. M., Araújo J. P., Silva A. F.: Electrodeposition of an ultrathin TiO_2 coating using a deep eutectic solvent based on choline chloride. Thin Solid Films, **645**, 391–398 (2018). https://doi.org/10.1016/j.tsf.2017.11.005

[23] Pereira N. M., Pereira C. M., Araújo J. P., Silva A. F.: Zinc electrodeposition from deep eutectic solvent containing organic additives. Journal of Electroanalytical Chemistry, **801**, 545–551 (2017). https://doi.org/10.1016/j.jelechem.2017.08.019

[24] Ferreira E. S. C., Pereira C. M., Silva A. F.: Electrochemical studies of metallic chromium electrodeposition from a Cr(III) bath. Journal of Electroanalytical Chemistry, **707**, 52–58 (2013). https://doi.org/10.1016/j.jelechem.2013.08.005

[25] Salomé S., Pereira N. M., Ferreira S. M., Pereira C. M., Silva A. F.: Tin electrodeposition from choline chloride based solvent: Influence of the hydrogen bond donors. Journal of Electroanalytical Chemistry, **703**, 80–87 (2013). https://doi.org/10.1016/j.jelechem.2013.05.007

[26] Mota-Morales J. D., Sánchez-Leija R. J., Carranza A., Pojman J. A., del Monte F., Luna-Bárcenas G.: Free-radical polymerizations of and in deep eutectic solvents: Green synthesis of functional materials. Progress in Polymer Science, **78**, 139–153 (2018). https://doi.org/10.1016/j.progpolymsci.2017.09.005

[27] Carriazo D., Serrano M. C., Gutiérrez M. C., Ferrer M. L., del Monte F.: Deep-eutectic solvents playing multiple roles in the synthesis of polymers and related materials. Chemical Society Reviews, **14**, 4996–5014 (2012). https://doi.org/10.1039/c2cs15353j

[28] del Monte F., Carriazo D., Serrano M. C., Gutiérrez M. C., Ferrer M. L.: Deep eutectic solvents in polymerizations: A greener alternative to conventional syntheses. ChemSusChem, **7**, 999–1009 (2014). https://doi.org/10.1002/cssc.201300864

[29] Zhang Q., Vigier K. O., Royer S., Jérôme F.: Deep eutectic solvents: Syntheses, properties and applications. Chemical Society Reviews, **21**, 7108–7147 (2012). https://doi.org/10.1039/C2CS35178A

[30] Lee D. W., Jin M. H., Park J. H., Lee Y. J., Choi Y. C., Park J. C., Chun D. H.: Alcohol and water free synthesis of mesoporous silica using deep eutectic solvent as a template and solvent and its application as a catalyst support for formic acid dehydrogenation. ACS Sustainable Chemistry and Engineering, **6**, 12241–12250 (2018). https://doi.org/10.1021/acssuschemeng.8b02606

[31] Dodgson K. S.: Determination of inorganic sulphate in studies on the enzymic and non-enzymic hydrolysis of carbohydrate and other sulphate esters. Biochemical Journal, **78**, 312–319 (1957).

[32] Gandhi R. R., Gowri S., Suresh J., Sundrarajan M.: Ionic liquids assisted synthesis of ZnO nanostructures: Controlled size, morphology and antibacterial properties. Journal of Materials Science and Technology, **29**, 533–538 (2013). https://doi.org/10.1016/j.jmst.2013.03.007

[33] Hammond O. S., Bowron D. T., Jackson A. J., Arnold T., Sanchez-Fernandez A., Tsapatsaris N., Sakai V. G., Edler J. K.: Resilience of malic acid natural deep eutectic solvent nanostructure to solidification and hydration. The Journal of Physical Chemistry B, **121**, 7473–7483 (2017). https://doi.org/10.1021/acs.jpcb.7b05454

[34] Dai Y., Witkamp G. J., Verpoorte R., Choi Y. H.: Tailoring properties of natural deep eutectic solvents with water to facilitate their applications. Food Chemistry, **187**, 14–19 (2015). https://doi.org/10.1016/j.foodchem.2015.03.123

[35] Choi H., Kim Y. J., Varma R. S., Dionysiou D. D.: Thermally stable nanocrystalline TiO_2 photocatalysts synthesized via sol–gel methods modified with ionic liquid and surfactant molecules. Chemistry of Materials, **18**, 5377–5384 (2006). https://doi.org/10.1021/cm0615626

[36] Foot M., Mulholland M.: Classification of chondroitin sulfate A, chondroitin sulfate C, glucosamine hydrochloride and glucosamine 6 sulfate using chemometric techniques. Journal of Pharmaceutical and Biomedical Analysis, **38**, 397–407 (2005). https://doi.org/10.1016/j.jpba.2005.01.026

[37] Choi J. I., Lee C. S. G., Han S. J., Cho M., Lee P. C.: Effect of gamma irradiation on the structure of fucoidan. Radiation Physics and Chemistry, **100**, 54–58 (2014). https://doi.org/10.1016/j.radphyschem.2014.03.018

[38] He Q., Shi J., Chen F., Zhu M., Zhang L.: An anticancer drug delivery system based on surfactant-templated mesoporous silica nanoparticles. Biomaterials, **31**, 3335–3346 (2010). https://doi.org/10.1016/j.biomaterials.2010.01.015

[39] Bai G., Catita J. A. M., Nichifor M., Bastos M.: Microcalorimetric evidence of hydrophobic interactions between hydrophobically modified cationic polysaccharides and surfactants of the same charge. Journal of Physical Chemistry B, **111**, 11453–11462 (2007). https://doi.org/10.1021/jp073530r

[40] Bao H., Li L., Gan L. H., Zhang H.: Interactions between ionic surfactants and polysaccharides in aqueous solutions. Macromolecules, **41**, 9406–9412 (2008). https://doi.org/10.1021/ma801957v

[41] Azizian S.: Kinetic models of sorption: A theoretical analysis. Journal of Colloid and Interface Science, **276**, 47–52 (2004). https://doi.org/10.1016/j.jcis.2004.03.048

[42] Da´na E.: Adsorption of heavy metals on functionalized-mesoporous silica: A review. Microporous and Mesoporous Materials, **247**, 145–157 (2017). https://doi.org/10.1016/j.micromeso.2017.03.050

[43] Ngah W. S. W., Fatinathan S.: Pb(II) biosorption using chitosan and chitosan derivatives beads: Equilibrium, ion exchange and mechanism studies. Journal of Environmental Science, **22**, 338–346 (2010). https://doi.org/10.1016/S1001-0742(09)60113-3

[44] Li G., Zhao Z., Liu J., Jiang G.: Effective heavy metal removal from aqueous systems by thiol functionalized magnetic mesoporous silica. Journal of Hazardous Materials, **192**, 277–283 (2011). https://doi.org/10.1016/j.jhazmat.2011.05.015

[45] Fan L., Luo C., Sun M., Li X., Qiu H.: Highly selective adsorption of lead ions by water-dispersible magnetic chitosan/graphene oxide composites. Colloids and Surfaces B, **103**, 523–529 (2013). https://doi.org/10.1016/j.colsurfb.2012.11.006

[46] Heidari A., Younesi H., Mehraban Z.: Removal of Ni(II), Cd(II), and Pb(II) from a ternary aqueous solution by amino functionalized mesoporous and nano mesoporous silica. Chemical Engineering Journal, **153**, 70–79 (2009). https://doi.org/10.1016/j.cej.2009.06.016

[47] Liu Y., Liu Z., Gao J., Dai J., Han J., Wang Y., Xie J., Yan Y.: Selective adsorption behavior of Pb(II) by mesoporous silica SBA-15-supported Pb(II)-imprinted polymer based on surface molecularly imprinting technique. Journal of Hazardous Materials, **186**, 197–205 (2011). https://doi.org/10.1016/j.jhazmat.2010.10.105

[48] Lata S., Singh P. K., Samadder S. R.: Regeneration of adsorbents and recovery of heavy metals: A review. International Journal of Environmental Science and Technology, **12**, 1461–1478 (2015). https://doi.org/10.1007/s13762-014-0714-9